Published in final edited form as:
Curr Opin Biotechnol. 2009 February ; 20(1): 111–118. doi:10.1016/j.copbio.2009.02.007.

Fourier-domain optical coherence tomography: recent advances toward clinical utility

Brett E Bouma, **Seok-Hyun Yun**, **Benjamin J Vakoc**, **Melissa J Suter**, and **Guillermo J Tearney**
Wellman Center for Photomedicine, Massachusetts General Hospital, Harvard Medical School, Harvard-MIT Division of Health Sciences and Technology, MGH, BAR 701, 40 Blossom Street, Boston, MA 02114, United States

Abstract

With the advent of Fourier-domain techniques, optical coherence tomography (OCT) has advanced from high-resolution 'point' imaging over small fields-of-view to comprehensive microscopic imaging over three-dimensional volumes that are comparable to the dimensions of luminal internal organs. This advance has required the development of new lasers, improved spectrometers, minimally invasive catheters and endoscopes, and novel optical and signal processing strategies. In recent cardiovascular, ophthalmic, and gastrointestinal clinical studies, the capabilities of Fourier-domain OCT have enabled a new paradigm for diagnostic screening of large tissue areas, which addresses the shortcomings of existing technologies and focal biopsy.

Introduction

Optical coherence tomography (OCT) was originally developed for imaging the human retina as a means for diagnosing pathologic changes at an early phase [1,2]. The clinical adoption of OCT in ophthalmology is now well established and commercial systems are in routine use for research and clinical practice. In comparison, the translation of OCT for other clinical applications has lagged; although the first demonstration of catheter-based OCT for imaging internal organs was published in 1997 [3], the technology has not been adopted for routine practice. Recent advances, however, promise to change this status.

In the field of cardiology, there is a pressing need for improved characterization of coronary pathology in order to better understand factors associated with heart attack and to develop and guide the deployment of better therapeutic strategies. The resolution and image contrast of OCT are attractive for this application and suitable catheters have been developed that provide minimally invasive access to the main coronary arteries. The challenge, however, has been that blood is nearly opaque to light and strategies to either occlude flow or to displace blood through the injection of a transparent liquid such as saline can be applied for only a few seconds without risk of ischemia. Early clinical pilot studies with OCT demonstrated excellent image quality, but since the acquisition rate was limited to a few frames per second, only discrete locations

Corresponding author: Bouma, Brett E (bouma@helix.mgh.harvard.edu), Yun, Seok-Hyun (syun@hms.harvard.edu), Vakoc, Benjamin J (bvakoc@partners.org), Suter, Melissa J (msuter@partners.org) and Tearney, Guillermo J (tearney@helix.mgh.harvard.edu).
This review comes from a themed issue on Analytical biotechnology Edited by Christopher Contag and Kevin Eliceiri

Conflicts of interest

BEB and GJT: Research sponsored partly by Terumo Corporation, Olympus Corporation, Air Liquide, and Boston Scientific. Co-inventors on patents licensed to LightLab Imaging and Carl Zeiss Meditec, through MIT. Co-inventors on patents licensed to Terumo Corporation and Nidec Corporation, through MGH.
BJV and SHY: Co-inventors on patents licensed to Terumo Corporation and Nidec Corporation, through MGH.

within the coronary arteries could be visualized. The recent advance of new Fourier-domain strategies for OCT has overcome this limitation by increasing imaging speeds to more than 100 frames per second. This increase in the imaging speed allows long coronary artery segments to be imaged following a brief, non-occlusive injection of saline through the guiding catheter. As commercial Fourier-domain OCT systems become available, it is likely that the forecast for adoption of this technology in cardiology will dramatically change.

The benefits of Fourier-domain OCT may have a similar significance for endoscopic and laparoscopic applications in screening and surveillance for early neoplastic changes. In these applications, the rationale for high-speed acquisition is to enable wide-field imaging of large luminal surface areas in the exploration for early stage, focal disease. Although excisional biopsy can be safe and effective for focal diagnosis, the ability to survey large tissue volumes noninvasively could revolutionize diagnostic procedures. Current studies are, for example, investigating Fourier-domain OCT for diagnostic imaging of the entire distal esophagus with a resolution approaching that of histopathology. The following review will focus on the recent technical advances that have enabled Fourier-domain techniques and will highlight clinical applications for which this technology may have the most significant impact.

Time-domain OCT

Interferometric methods for length measurements have been used pervasively in the physical sciences for over a century. By measuring the cross-correlation between an electric field reflected from a target and a coherent replica of the original field, distances can be readily measured with a precision well below a single wavelength. Measurements can be performed using temporal delay or wavelength as the variable coordinate and many interferometer topologies have been exploited [4,5]. In the early 1990s, interferometry was investigated for length measurements in the human eye [6], exploiting the ability of this approach to determine the range to multiple reflection sites along a single optical axis. Not long after this, transverse scanning of the optical beam was implemented and the interferometric signal strength was converted to a color-scale or gray-scale to provide a cross-sectional image [1,2]. This approach has become recognized as time-domain optical coherence tomography (OCT), conventionally referring to an interferometric imaging system in which the reference delay is scanned.

In many respects, ophthalmic imaging is unique in comparison with other biological applications; the anterior portion of the eye and the vitreous are highly transparent with little optical scattering, the eye can be stabilized effectively, and the eye can be directly accessed with optical instrumentation. Recognizing the potential of OCT for imaging through minimally invasive catheters and endoscopes, however, research in the mid-1990s was directed to resolve several deficiencies of the prototype ophthalmic OCT systems. Improved resolution, approaching 1 μm, was achieved through the use of ultrafast mode locked lasers [7–9]. Imaging speed, required to overcome motion artifacts arising from respiration, cardiovascular function, and peristalsis, was increased 10-fold through the use of a phase-controlled rapid scanning delay line [10]. Since the dominant mechanism limiting the depth of penetration of the conventional near infrared (~800 nm) ophthalmic systems was optical scattering rather than absorption, the use of infrared light near 1300 nm improved imaging depths to a few mm in most biological tissues. [11,12] Although this is shallow in comparison with other clinical imaging modalities, such as ultrasound or diffuse-light techniques, it is sufficient for many biological and clinical applications, provided that minimally invasive probes can be utilized to deliver light to [13] and collect light from the tissue of interest. Appropriate probes were developed for intravascular [14], laparoscopic [15], and endoscopic delivery [13,16]. Combining these advances, small animal internal organ imaging was demonstrated for the first time *in vivo* in 1997 [3].

Shortly after the first demonstration of imaging *in vivo* with OCT, portable systems were developed and human clinical pilot studies were conducted to evaluate imaging in the upper and lower gastrointestinal tract [16–18], the common bile duct [19], the lung and airways [20], the cervix [21], the bladder [22,23], the larynx [24], and the coronary arteries [25–31]. These early studies showed that the resolution and contrast provided by OCT were significantly better than could be provided by conventional imaging techniques such as ultrasound and that a spectrum of pathologic states could be identified. The widespread adoption of OCT into clinical practice, however, did not follow. One significant barrier inhibiting adoption was the focal nature of OCT imaging; the catheter or endoscope probe was placed at discrete locations and cross-sectional images were obtained. The resulting diagnostic information could never therefore substantially exceed that provided by excisional biopsy.

In 2003, nearly simultaneous reports were published that demonstrated theoretically [32•, 33•,34•] and experimentally [35•,36,37•] that shifting from the time-domain of conventional OCT to the Fourier-domain, in which the electric field cross-correlation is sampled as a function of wavenumber, provides several orders of magnitude improvement in detection sensitivity. The significance of this finding for clinical applications was enormous since it enabled dramatically faster imaging speeds and therefore allowed imaging over very large fields of view. [38••]

Fourier-domain OCT

Even at the inception of OCT, it was well known that interferometric ranging could be performed using wavenumber as the variable coordinate. In practice, this could be achieved either through the use of a wavelength-swept light source and a standard photodiode receiver or with a broadband light source and a spectrometer. In both cases, the acquired signal is the integrated spectrum of the light source, superimposed by fringes whose frequency encodes the pathlength imbalance of the interferometer. Through Fourier transformation, the sample reflectance as a function of depth is obtained. The terminology associated with these different configurations has not been standardized. Typically, the original coherence-domain OCT is now referred to as time-domain OCT. The configuration using a spectrometer (Figure 1a) has been referred to as spectral radar [39] and spectral-domain OCT; and the configuration using the wavelength-swept laser (Figure 1b) has been referred to as frequency-domain OCT, optical frequency domain imaging (OFDI), and swept-source OCT.

The detection sensitivity in Fourier-domain OCT is enhanced because the receiver registers reflected light from all depth-points in the sample simultaneously over the duration of one complete axial profile. In time-domain OCT, the short temporal coherence of the light source is exploited to reject the reflected light from all but one depth point and to successively read reflection as a function of depth until a complete axial profile is collected. As a result, the enhancement of signal-to-noise ratio in Fourier-domain systems is given roughly by the number of axial points in an image. In either configuration, the theoretical enhancement of sensitivity can readily be made to be in the order of 100–1000. In practice, many factors can prevent realization of this improvement. In particular, backscattering arising in the optical fiber path of the interferometer sample arm gives rise to an elevated noise floor, but systems with enhancements of between 50 and 100 have been demonstrated.

Increased detection sensitivity could be utilized to reduce the optical power incident upon the sample while still achieving image penetration to the multiple-scattering limit. Although this advantage may be useful in ophthalmology, most research groups have exploited the increased sensitivity of Fourier-domain systems to achieve higher imaging speed so that larger areas of the retina can be imaged without motion artifacts. In spectral-domain OCT, this requires a high-speed linear detector array, comprising more than 1000 individual elements. Silicon-base line-

scan cameras were the first to be integrated into spectral-domain systems and provided readout rates of approximately 40 kHz. In comparison, InGaAs cameras, appropriate for use with 1.3 μm light sources were less mature, providing fewer pixels and slower readout rates. In addition to the line-scan camera, spectral-domain OCT system required the development of appropriate spectrometers [35•,40•] but leveraged from existing broadband light sources that were already developed for time-domain OCT.

The practical realization of high-speed frequency-domain OCT systems required the development of a new wavelength-swept laser with a narrow instantaneous linewidth, a broad tuning range, a linear sweep, and a high average power. Previous tunable lasers provided insufficient spectral range, sweep repetition rate, and power. The first demonstration of high-speed imaging relied on a novel laser configuration comprising a fiber optic ring, a semiconductor optical amplifier, and a wavelength filter constructed using a polygon scanner [41]. Subsequent improvements using the same general design yielded 115 kHz repetition rate scanning [42] and wavelength ranges extending over 145 nm centered at 1.3 μm [43]. At high-speed operation, the spectral sweep rate of the filter becomes large with respect to the resonator round-trip delay. Although the most straightforward solution to this limitation would be to miniaturize the cavity, another elegant solution is to synchronize the round trip time of the resonator with the filter [44]. In this approach, recently termed Fourier-domain mode locking [45], a long resonator is used so that on each round trip through the cavity, individual wavelengths return to the filter as the filter returns to the matching wavelength during the successive scan. Repetition rates as high as 370 kHz have been demonstrated in this way [46••]. Presently, the maximum imaging speed that can be achieved with frequency-domain OCT is limited by digital data transfer and storage.

One technical challenge to Fourier-domain approaches is the degeneracy between positive and negative depths in the sample; only the magnitude of depth is mapped to fringe frequency. A simple solution, applicable to frequency-domain systems, is to apply a frequency offset, through the use of an acousto-optic modulator, to shift the signal frequency corresponding to zero relative delay to an RF carrier [47]. This approach yields a doubling of the effective ranging depth. Alternatively, the intensity and quadrature of the Fourier-domain signal can be acquired to overcome the depth degeneracy [48–54].

With the availability of robust and portable Fourier-domain systems, clinical studies that exploit wide-field microscopic imaging have commenced. Using a frequency-domain system operating at 40 kHz A-line rate, endoscopic imaging of the entire distal esophagus in human subjects has been demonstrated (Figure 3). [55••] In contrast to previous endoscopic OCT studies in which diagnostic imaging was restricted to a similar field-of-view provided by excisional biopsy, the new generation systems are able to provide diagnostic information not accessible by biopsy. In ophthalmology, the high speed of Fourier-domain OCT has permitted comprehensive mapping of the microscopic structure of the retina. [56–58,59••] In the field of cardiology where intravascular OCT has been frustrated by the opacity of blood, Fourier-domain systems have yielded significant advances. Using only intermittent injection of transparent fluid to displace blood from coronary arteries for a few seconds, volumetric images have been obtained for entire coronaries (Figure 2). [38••,60••] This advance may provide dramatic improvements in understanding coronary atherosclerosis and response to intravascular interventions such as angioplasty and stenting.

Conclusions

The recent development of high-speed imaging systems based on OCT principles will undoubtedly change the landscape of clinical implementation and adoption. While preserving the resolution and contrast of time-domain OCT, Fourier-domain systems enable

comprehensive imaging over large fields of view and address the primary limitation of early OCT technology.

Although InGaAs linescan camera technology is presently advancing to rival the capabilities of the more mature silicon-based detectors, it is likely that the present division of applications between spectral-domain systems and frequency-domain systems will continue for some time. In ophthalmic applications, the preferred wavelength for imaging is near 800 nm owing to the relatively low absorption at this wavelength in the anterior eye and vitreous. Since the development of rapidly swept lasers at 800 nm is limited by the lack of appropriate semiconductor sources and since relatively inexpensive silicon-based cameras are already available that support imaging speeds approaching 100 frames per second, it is likely that spectral-domain OCT will remain dominant in ophthalmology. For catheter-based and endoscope-based imaging where low-loss fibers are used to deliver the light directly to the target organs, 1300 nm is preferable and results in greater imaging penetration within tissue. Since wavelength swept laser technology is now readily available for this spectral region and since the continued advancement of new high-speed cameras will require significant investment, frequency-domain OCT appears to be the most effective strategy. Additionally, frequency-domain systems are less prone to signal fading associated with optical phase variations in the optical fibers of catheters and endoscopes. Since appropriate technical strategies for Doppler and polarization-sensitive imaging have been developed for both the approaches, vasculature and birefringence imaging applications may not be a primary consideration in selecting between the two platforms.

Perhaps the most important area of continued technical development for the new generation OCT systems will be in signal and image processing. Current systems are capable of producing data rates approaching 1 GB/s. New strategies will be required for fast processing that includes interpolation and Fourier transformation. Dedicated digital signal processing such as field programmable gate array processing may yield effective strategies for computation and reduction of data volume before archiving. Additionally, new algorithms will be required for interpreting images for diagnosis or for preselecting portions of datasets for review by human experts.

Future work will also undoubtedly lead to the integration of techniques for expanding contrast and molecular specificity to Fourier-domain OCT. Many of the methods that were developed for time-domain OCT, including Doppler flow detection [61,62], birefringence characterization [63–65], and biochemical contrast [66,67•,68–72] can be directly translated into the new platforms. Indeed, methods for flow visualization [73–76] and polarization sensitivity [73,77–81] have already been demonstrated in Fourier-domain systems.

Although the path from the first OCT prototypes to the present capabilities has been long, the ground work to support adoption of the new Fourier-domain systems has heightened awareness in the biological and clinical communities and may be a factor in rapid commercialization. At present, there are more than a dozen companies with Fourier-domain systems either recently available or on the near-term horizon and prospects for wide spread application are excellent.

Acknowledgements

The authors gratefully acknowledge the following collaborators who have helped to shape the perspectives and technical analysis presented in this review: M Shishkov, JF de Boer, WY Oh, A Desjardins, BH Park, and RC Chan. BE Bouma and GJ Tearney are supported by the National Institutes of Health, Grants R01CA103769, R01HL076398, and R33-CA125560. SH Yun is supported by the National Institutes of Health, Grant R33CA110130. BJ Vakoc is supported by National Institutes of Health, Grant K25-CA127465.

References and recommended reading

Papers of particular interest, published within the period of review, have been highlighted as:

• of special interest

•• of outstanding interest

1. Huang D, Swanson EA, Lin CP, Schuman JS, Stinson WG, Chang W, Hee MR, Flotte T, Gregory K, Puliafito CA, et al. Optical coherence tomography. Science 1991;254:1178–1181. [PubMed: 1957169]
2. Fercher AF, Hitzenberger CK, Drexler W, Kamp G, Sattmann H. *In vivo* optical coherence tomography. Am J Ophthalmol 1993;116:113–115. [PubMed: 8328536]
3. Tearney GJ, Brezinski ME, Bouma BE, Boppart SA, Pitris C, Southern JF, Fujimoto JG. *In vivo* endoscopic optical biopsy with optical coherence tomography. Science 1997;276:2037–2039. [PubMed: 9197265]
4. Takada K, Yokohama I, Chida K, Noda J. New measurement system for fault location in optical waveguide devices based on interferometric technique. Appl Opt 1987;26:1603–1606.
5. Youngquist RC, Carr S, Davies DEN. Optical coherence domain reflectometry: a new optical evaluation technique. Opt Lett 1987;12:158–160. [PubMed: 19738824]
6. Fercher AF, Mengedoht K, Werner W. Eye-length measurement by interferometry with partially coherent-light. Opt Lett 1988;13:186–188. [PubMed: 19742022]
7. Bouma B, Tearney GJ, Boppart SA, Hee MR, Brezinski ME, Fujimoto JG. High-resolution optical coherence tomographic imaging using a mode-locked ti:Al_2o_3 laser source. Opt Lett 1995;20:1486–1488.
8. Bouma BE, Tearney GJ, Bilinsky IP, Golubovic B, Fujimoto JG. Self-phase-modulated kerr-lens mode-locked cr:Forsterite laser source for optical coherence tomography. Opt Lett 1996;21:1839–1841.
9. Povazay B, Bizheva K, Unterhuber A, Hermann B, Sattmann H, Fercher AF, Drexler W, Apolonski A, Wadsworth WJ, Knight JC, et al. Submicrometer axial resolution optical coherence tomography. Opt Lett 2002;27:1800–1802. [PubMed: 18033368]
10. Tearney GJ, Bouma BE, Fujimoto JG. High-speed phase- and group-delay scanning with a grating-based phase control delay line. Opt Lett 1997;22:1811–1813. [PubMed: 18188374]
11. Fujimoto JG, Brezinski ME, Tearney GJ, Boppart SA, Bouma B, Hee MR, Southern JF, Swanson EA. Optical biopsy and imaging using optical coherence tomography. Nat Med 1995;1:970–972. [PubMed: 7585229]
12. Schmitt JM, Knuttel A, Yadlowsky M, Eckhaus MA. Optical-coherence tomography of a dense tissue: statistics of attenuation and backscattering. Phys Med Biol 1994;39:1705–1720. [PubMed: 15551540]
13. Bouma BE, Tearney GJ. Power-efficient nonreciprocal interferometer and linear-scanning fiber-optic catheter for optical coherence tomography. Opt Lett 1999;24:531–533. [PubMed: 18071562]
14. Tearney GJ, Boppart SA, Bouma BE, Brezinski ME, Weissman NJ, Southern JF, Fujimoto JG. Scanning single-mode fiber optic catheter-endoscope for optical coherence tomography. Opt Lett 1996;21:543–545.
15. Boppart SA, Bouma BE, Pitris C, Tearney GJ, Fujimoto JG, Brezinski ME. Forward-imaging instruments for optical coherence tomography. Opt Lett 1997;22:1618–1620. [PubMed: 18188315]
16. Sergeev A, Gelikonov V, Gelikonov G, Feldchtein F, Kuranov R, Gladkova N, Shakhova N, Snopova L, Shakhov A, Kuznetzova I, et al. *In vivo* endoscopic oct imaging of precancerand cancer states of human mucosa. Opt Exp 1997;1:432–440.
17. Bouma BE, Tearney GJ, Compton CC, Nishioka NS. High-resolution imaging of the human esophagus and stomach *in vivo* using optical coherence tomography. Gastrointest Endosc 2000;51:467–474. [PubMed: 10744824]
18. Sivak JMV, Kobayashi K, Izatt JA, Rollins AM, Ung-runyawee R, Chak A, Wong RCK, Isenberg GA, Willis J. High-resolution endoscopic imaging of the gi tract using optical coherence tomography. Gastrointest Endosc 2000;51:474–479. [PubMed: 10744825]

19. Poneros JM, Tearney GJ, Shishkov M, Kelsey PB, Lauwers GY, Nishioka NS, Bouma BE. Optical coherence tomography of the biliary tree during ercp. Gastrointest Endosc 2002;55:84–88. [PubMed: 11756925]

20. Mikhail-Hanna N, Mukai D, El-Abbadi NH, Jung WG, Mina-Araghi R, Chen ZP, Colt H, Brenner M. Optical coherence tomography of the lung and lower airway. Am Coll Chest Physicians 2003:77S.

21. Escobar PF, Belinson JL, White A, Shakhova NM, Feldchtein FI, Kareta MV, Gladkova ND. Diagnostic efficacy of optical coherence tomography in the management of preinvasive and invasive cancer of uterine cervix and vulva. Int J Gynecol Cancer 2004;14:470–474. [PubMed: 15228420]

22. Hermes B, Spoler F, Naami A, Bornemann J, Forst M, Grosse J, Jakse G, Knuchel R. Visualization of the basement membrane zone of the bladder by optical coherence tomography: feasibility of noninvasive evaluation of tumor invasion. Urology 2008;72:677–681. [PubMed: 18455778]

23. Zagaynova EV, Streltsova OS, Gladkova ND, Snopova LB, Gelikonov GV, Feldchtein FI, Morozov AN. *In vivo* optical coherence tomography feasibility for bladder disease. J Urol 2002;167:1492–1496. [PubMed: 11832776]

24. Burns JA, Zeitels SM, Anderson RR, Kobler JB, Pierce MC, de Boer JF. Imaging the mucosa of the human vocal fold with optical coherence tomography. Ann Publ Co 2005:671–676.

25. Jang I-K, Tearney GJ, Bouma BE. Visualization of tissue prolapse between coronary stent struts by optical coherence tomography: comparison with intravascular ultrasound. Circulation 2001;104:2754. [PubMed: 11723031]

26. Grube E, Gerckens U, Buellesfeld L, Fitzgerald PJ. Intracoronary imaging with optical coherence tomography—a new high-resolution technology providing striking visualization in the coronary artery. Circulation 2002;106:2409–2410. [PubMed: 12403675]

27. Jang IK, Tearney GJ, MacNeill BM, Takano M, Moselewski F, Iftimia N, Shishkov M, Houser SL, Aretz HT, Halpern EF, et al. *In vivo* characterization of coronary atherosclerotic plaque using optical coherence tomography. Circulation 2005;111:1551–1555. [PubMed: 15781733]

28. Regar E, van Beusekom HMM, van der Giessen WJ, Serruys PW. Optical coherence tomography findings at 5-year follow-up after coronary stent implantation. Circulation 2005;112:E345–E346. [PubMed: 16330689]

29. Kume T, Akasaka T, Kawamoto T, Watanabe N, Toyota E, Sukmawan R, Sadahira Y, Yoshida K. Visualization of neointima formation by optical coherence tomography. Int Heart J 2005;46:1133–1136. [PubMed: 16394609]

30. Fujii K, Masutani M, Okumura T, Kawasaki D, Akagami T, Ezumi A, Sakoda T, Masuyama T, Ohyanagi M. Frequency and predictor of coronary thin-cap fibroatheroma in patients with acute myocardial infarction and stable angina pectoris a 3-vessel optical coherence tomography study. J Am Coll Cardiol 2008;52:787–788. [PubMed: 18718429]

31. Guagliumi G, Sirbu V. Optical coherence tomography: high resolution intravascular imaging to evaluate vascular healing after coronary stenting. Catheter Cardiovasc Interv 2008;72:237–247. [PubMed: 18655155]

32. Choma M, Sarunic M, Yang C, Izatt J. Sensitivity advantage of swept source and fourier domain optical coherence tomography. Opt Exp 2003;11:2183–2189.2189 Along with references [33•] and [34•], this manuscript provided a comprehensive theoretical analysis demonstrating the improvement in signal detection sensitivity provided by Fourier-domain OCT relative to time-domain OCT.

33. de Boer JF, Cense B, Park BH, Pierce MC, Tearney GJ, Bouma BE. Improved signal-to-noise ratio in spectral-domain compared with time-domain optical coherence tomography. Opt Lett 2003;28:2067–2069.2069 [PubMed: 14587817] Along with references [32•] and [34•], this manuscript provided a comprehensive theoretical analysis demonstrating the improvement in signal detection sensitivity provided by Fourier-domain OCT relative to time-domain OCT.

34. Leitgeb R, Hitzenberger C, Fercher A. Performance of fourier domain vs. Time domain optical coherence tomography. Opt. Express 2003;11:889–894.894 [PubMed: 19461802] Along with references [32•] and [33•], this manuscript provided a comprehensive theoretical analysis demonstrating the improvement in signal detection sensitivity provided by Fourier-domain OCT relative to time-domain OCT.

35. Wojtkowski M, Bajraszewski T, Targowski P, Kowalczyk A. Real-time *in vivo* imaging by high-speed spectral optical coherence tomography. Opt Lett 2003;28:1745–1747.1747 [PubMed:

14514087] The authors describe the use of spectral-domain OCT for acquiring individual axial scans in 64 μs and confirm the ability to preserve high-resolution and deep imaging penetration.

36. Yun SH, Tearney GJ, Bouma BE, Park BH, de Boer JF. High-speed spectral-domain optical coherence tomography at 1.3 μm wavelength. Opt Exp 2003;11:3598–3604.
37. Yun SH, Tearney GJ, de Boer JF, Iftimia N, Bouma BE. High-speed optical frequency-domain imaging. Opt Exp 2003;11:2953–2963.2963 The authors describe the first high-speed frequency-domain OCT system based on a novel wavelength swept laser source.
38. Yun SH, Tearney GJ, Vakoc BJ, Shishkov M, Yelin R, Oh WY, Desjardins A, Chan RC, Yelin D, Evans JA, et al. Comprehensive volumetric optical microscopy *in vivo*. Nat Med 2006;12:1429–1433.1433 [PubMed: 17115049] Catheter-based imaging of internal organs was demonstrated for the first time *in vivo* using frequency-domain OCT. The fast acquisition speed of the imaging system enabled comprehensive imaging over large segments of the esophagus and coronary arteries in swine.
39. Hausler G, Lindner MW. coherence radar" and 'spectral radar'—new tools for dermatological diagnosis. J Biomed Opt 1998;3:21–31.
40. White B, Pierce M, Nassif N, Cense B, Park B, Tearney G, Bouma B, Chen T, de Boer J. *In vivo* dynamic human retinal blood flow imaging using ultra-high-speed spectral domain optical doppler tomography. Opt Exp 2003;11:3490–3497.3497 The authors report the development of a spectral-domain OCT system capable of acquiring axial scans at a sustained rate of 29 kHz.
41. Yun S, Boudoux C, Tearney G, Bouma B. High-speed wavelength-swept semiconductor laser with polygon-scanner-based wavelength filter. Opt Lett 2003;28:1981–1983. [PubMed: 14587796]
42. Oh WY, Yun SH, Tearney GJ, Bouma BE. 115 khz tuning repetition rate ultrahigh-speed wavelength-swept semiconductor laser. Opt Lett 2005;30:3159–3161. [PubMed: 16350273]
43. Oh WY, Yun SH, Tearney GJ, Bouma BE. Wide tuning range wavelength-swept laser with two semiconductor optical amplifiers. Photonics Technol Lett 2005;17:678–680.
44. Telle JM, Tang CL. Very rapid tuning of cw dye laser. Appl Phys Lett 1975;26:572–574.
45. Huber R, Wojtkowski M, Fujimoto JG. Fourier domain mode locking (fdml): a new laser operating regime and applications for optical coherence tomography. Opt Exp 2006;14:3225–3237.
46. Adler DC, Huber R, Fujimoto JG. Phase-sensitive optical coherence tomography at up to 370 000 lines per second using buffered fourier domain mode-locked lasers. Opt Lett 2007;32:626–628.628 [PubMed: 17308582] Using a Fourier-domain mode locked laser, wherein the wavelength filter repetition is synchronized with the laser resonator round-trip repetition, the authors demonstrate frequency-domain OCT with a depth-scanning rate of 370 kHz.
47. Yun SH, Tearney GJ, de Boer JF, Bouma BE. Removing the depth-degeneracy in optical frequency domain imaging with frequency shifting. Opt Exp 2004;12:4822–4828.
48. Sarunic MV, Choma MA, Yang CH, Izatt JA. Instantaneous complex conjugate resolved spectral domain and swept-source oct using 3 × 3 fiber couplers. Opt Exp 2005;13:957–967.
49. Vakoc BJ, Yun SH, Tearney GJ, Bouma BE. Elimination of depth degeneracy in optical frequency domain imaging through polarization-based optical demodulation. Opt Lett 2006;31:362–364. [PubMed: 16480209]
50. Bu P, Wang XZ, Sasaki O. Dynamic full-range fourier-domain optical coherence tomography using sinusoidal phase-modulating interferometry. Opt Eng 2007:46.
51. Sarunic MV, Applegate BE, Izatt JA. Real-time quadrature projection complex conjugate resolved fourier domain optical coherence tomography. Opt Lett 2006;31:2426–2428. [PubMed: 16880844]
52. Tao YK, Zhao M, Izatt JA. High-speed complex conjugate resolved retinal spectral domain optical coherence tomography using sinusoidal phase modulation. Opt Lett 2007;32:2918–2920. [PubMed: 17938652]
53. Leitgeb RA, Michaely R, Lasser T, Sekhar SC. Complex ambiguity-free fourier domain optical coherence tomography through transverse scanning. Opt Lett 2007;32:3453–3455. [PubMed: 18059964]
54. Mao YX, Sherif S, Flueraru C, Chang S. 3 × 3 mach-zehnder interferometer with unbalanced differential detection for full-range swept-source optical coherence tomography. Appl Opt 2008;47:2004–2010. [PubMed: 18425172]
55. Suter MJ, Vakoc BJ, Yachimski PS, Shishkov M, Lauwers GY, Mino-Kenudson M, Bouma BE, Nishioka NS, Tearney GJ. Comprehensive microscopy of the esophagus in human patients with

optical frequency domain imaging. Gastrointest Endosc 2008;68:745–753.753 [PubMed: 18926183] This manuscript describes the first use of high-speed, high-resolution Fourier-domain OCT for large area, three-dimensional imaging of the esophagus. Through the use of an endoscopic balloon probe and high-speed optical frequency domain imaging, the entire distal esophagus was imaged. The depth of imaging penetration was sufficient to visualize the full esophageal thickness.

56. Cense B, Nassif NA, Chen T, Pierce M, Yun SH, Park BH, Bouma BE, Tearney GJ, de Boer JF. Ultrahigh-resolution high-speed retinal imaging using spectral-domain optical coherence tomography. Opt Exp 2004;12:2435–2447.
57. Chen TC, Cense B, Miller JW, Rubin PAD, Deschler DG, Gragoudas ES, de Boer JF. Histologic correlation of *in vivo* optical coherence tomography images of the human retina. Am J Ophthalmol 2006;141:1165–1168. [PubMed: 16765704]
58. Kaluzny JJ, Wojtkowski M, Sikorski BL, Szkulmowski M, Szkulmowska A, Bajraszewski T, Fujimoto JG, Duker JS, Schuman JS, Kowalczyk A. Analysis of the outer retina reconstructed by high-resolution, three-dimensional spectral domain optical coherence tomography. Ophthalmic Surg Lasers Imaging 2008;39:S30–S36.
59. Lim JI, Tan O, Fawzi AA, Hopkins JJ, Gil-Flamer JH, Huang D. A pilot study of fourier-domain optical coherence tomography of retinal dystrophy patients. Am J Ophthalmol 2008;146:417–426.426 [PubMed: 18635153] The authors report results from a clinical study of retinal dystrophy using spectral-domain OCT to quantify macular inner retinal layer and macular outer retinal layer thicknesses. The high resolution of the imaging system allowed quantitative analysis of the anatomical retinal layers while the high speed of SD-OCT permitted imaging over large areas of the retina.
60. Tearney GJ, Waxman S, Shishkov M, Vakoc BJ, Suter MJ, Freilich MI, Desjardins AE, Oh WY, Bartlett LA, Rosenberg M, et al. Three-dimensional coronary artery microscopy by intracoronary optical frequency domain imaging: first-in-man experience. JACC Cardiovasc Imaging 2008;1:752–761.761 [PubMed: 19356512] Using optical frequency domain imaging, the authors demonstrate comprehensive intracoronary imaging in human patients. This is the first study demonstrating high-resolution cross-sectional and three-dimensional OCT imaging over long coronary segments.
61. Izatt JA, Kulkarni MD, Yazdanfar S, Barton JK, Welch AJ. *In vivo* bidirectional color doppler flow imaging of picoliter blood volumes using optical coherence tomography. Opt Lett 1997;22:1439–1441. [PubMed: 18188263]
62. Wang XJ, Milner TE, Nelson JS. Characterization of fluid flow velocity by optical doppler tomography. Opt Lett 1995;20:1337–1339.
63. Hee MR, Huang D, Swanson EA, Fujimoto JG. Polarization-sensitive low-coherence reflectometer for birefringence characterization and ranging. J Opt Soc Am B 1992;9:903–908.
64. de Boer JF, Milner TE, van Gemert MJC, Nelson JS. Two-dimensional birefringence imaging in biological tissue by polarization-sensitive optical coherence tomography. Opt Lett 1997;22:934–936. [PubMed: 18185711]
65. Everett MJ, Schoenenberger K, Colston JBW, Da Silva LB. Birefringence characterization of biological tissue by use of optical coherence tomography. Opt Lett 1998;23:228–230. [PubMed: 18084468]
66. Xu C, Ye J, Marks DL, Boppart SA. Near-infrared dyes as contrast-enhancing agents for spectroscopic opticalcoherence tomography. Opt Lett 2004;29:1647–1649. [PubMed: 15309847]
67. Applegate BE, Izatt JA. Molecular imaging of endogenous and exogenous chromophores using ground state recovery pump-probe optical coherence tomography. Opt Exp 2006;14:9142–9155.9155 The authors exploit transient absorption through pump-probe techniques to integrate molecular specificity with the high spatial resolution of OCT.
68. Jiang Y, Tomov I, Wang Y, Chen Z. Second-harmonic optical coherence tomography. Opt Lett 2004;29:1090–1092. [PubMed: 15181995]
69. Marks DL, Boppart SA. Nonlinear interferometric vibrational imaging. Phys Rev Lett 2004;92:123905-1–123905-4. [PubMed: 15089675]
70. Oldenburg AL, Gunther JR, Boppart SA. Imaging magnetically labeled cells with magnetomotive optical coherence tomography. Opt Lett 2005;30:747–749. [PubMed: 15832926]

71. Rao KD, Choma MA, Yazdanfar S, Rollins AM, Izatt JA. Molecular contrast in optical coherence tomography by use of a pump probe technique. Opt Lett 2003;28:340–342. [PubMed: 12659437]

72. Yang C, Choma MA, Lamb LE, Simon JD, Izatt JA. Protein-based molecular contrast optical coherence tomography withphytochrome as the contrast agent. Opt Lett 2004;29:1396–1398. [PubMed: 15233447]

73. Park BH, Pierce MC, Cense B, Yun SH, Mujat M, Tearney GJ, Bouma BE, de Boer JF. Real-time fiber-based multi-functional spectral-domain optical coherence tomography at 1.3 μm. Opt Exp 2005;13:3931–3944.

74. Szkulmowska A, Szkulmowski M, Kowalczyk A, Wojtkowski M. Phase-resolved doppler optical coherence tomography—limitations and improvements. Opt Lett 2008;33:1425–1427. [PubMed: 18594653]

75. Vakoc BJ, Yun SH, de Boer JF, Tearney GJ, Bouma BE. Phase-resolved optical frequency domain imaging. Opt Exp 2005;13:5483–5493.

76. An L, Wang RKK. *In vivo* volumetric imaging of vascular perfusion within human retina and choroids with optical micro-angiography. Opt Exp 2008;16:11438–11452.

77. Yamanari M, Makita S, Madjarova VD, Yatagai T, Yasuno Y. Fiber-based polarization-sensitive fourier domain optical coherence tomography using b-scan-oriented polarization modulation method. Opt Exp 2006;14:6502–6515.

78. Baumann B, Gotzinger E, Pircher M, Hitzenberger CK. Single camera based spectral domain polarization sensitive optical coherence tomography. Opt Exp 2007;15:1054–1063.

79. Oh WY, Yun SH, Vakoc BJ, Shishkov M, Desjardins AE, Park BH, de Boer JF, Tearney GJ, Bouma E. High-speed polarization sensitive optical frequency domain imaging with frequency multiplexing. Opt Exp 2008;16:1096–1103.

80. Yamanari M, Makita S, Yasuno Y. Polarization-sensitive swept-source optical coherence tomography with continuous source polarization modulation. Opt Exp 2008;16:5892–5906.

81. Oh WY, Vakoc BJ, Yun SH, Tearney GJ, Bouma BE. Single-detector polarization-sensitive optical frequency domain imaging using high-speed intra a-line polarization modulation. Opt Lett 2008;33:1330–1332. [PubMed: 18552948]

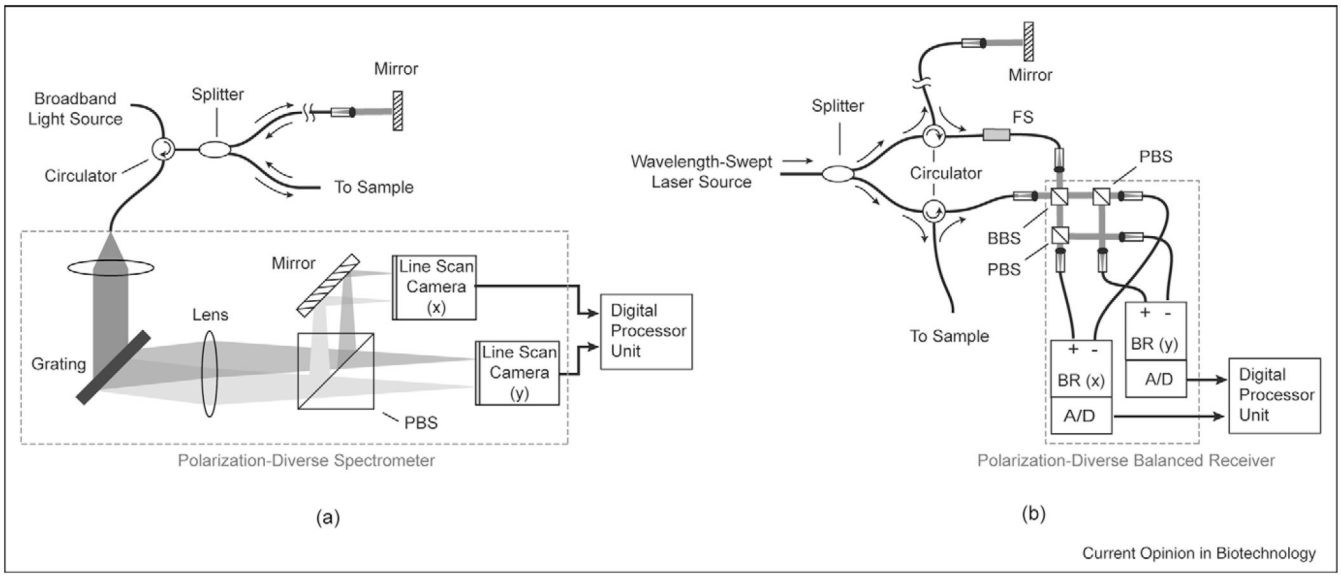

Figure 1.

Schematic layout of typical polarization-diverse Fourier-domain optical coherence tomography systems. **(a)** Spectral-domain systems rely on a broadband lightsource and a spectrometer as a detector. **(b)** In frequency-domain systems, the light source is a wavelength-swept laser and the receiver comprises single-element photodiodes. A frequency-shifter is typically used to resolve otherwise degenerate positive and negative depths relative to the reference arm pathlength. PBS: polarization beam splitter; BBS: broadband beam splitter.

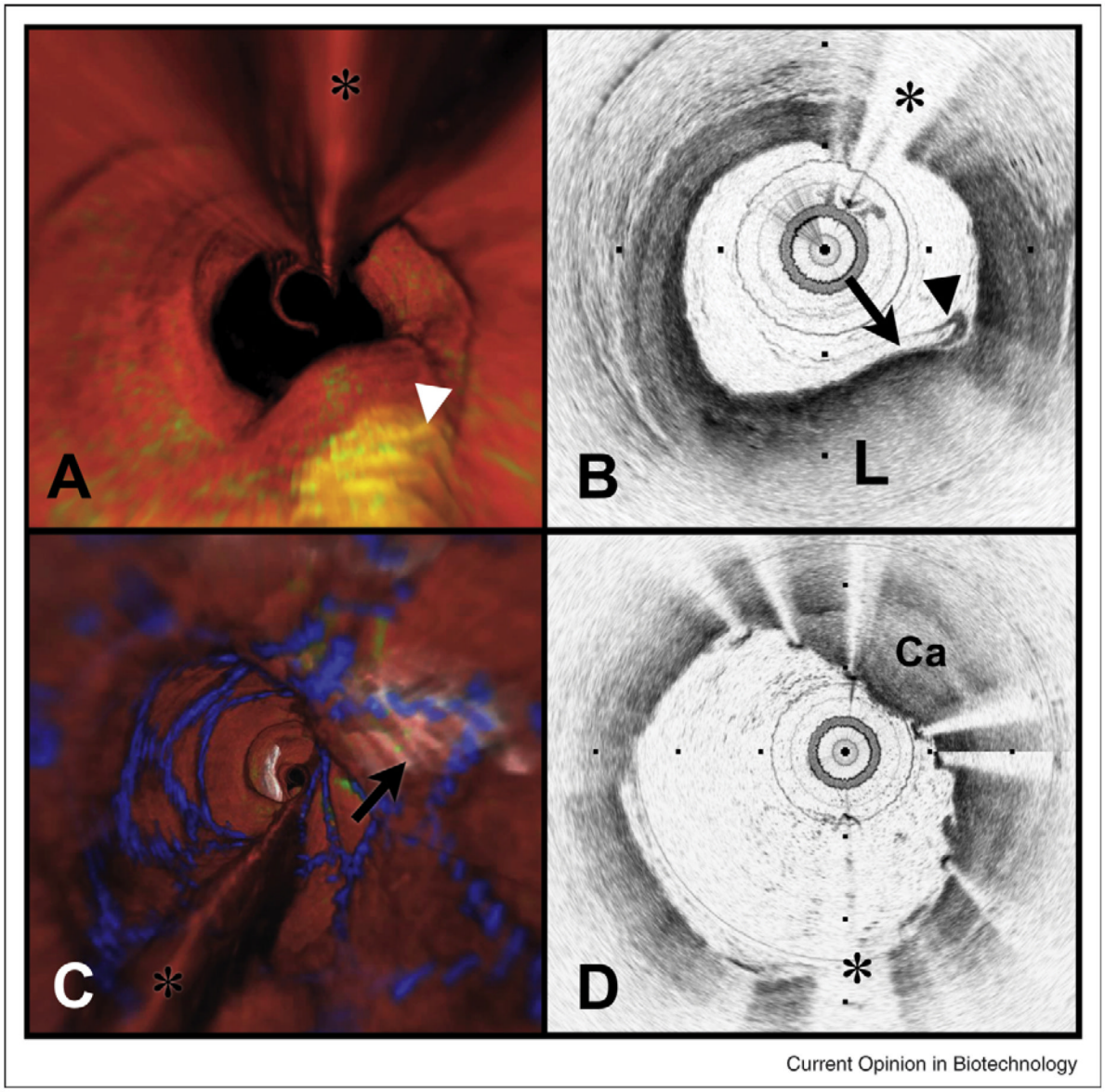

Figure 2.

Volumetric OFDI imaging of the human LAD coronary artery, obtained *in vivo*. **(A)** Fly-through rendering view (proximal-distal) of the OFDI dataset, acquired during a single purge of Lactated Ringers solution (3 ml/s), an imaging catheter pullback rate of 2.0 cm/s and at an image acquisition rate of 100 frames per second. The fly-through depicts a yellow, elevated lipid-rich lesion with scattered macrophages (green). **(B)** OFDI cross-sectional image obtained at the location of the white arrowhead in (A) demonstrates OFDI evidence of a thin-capped fibroatheroma, a lipid pool (L), a thin cap (black arrow), and a dense band of macrophages at the cap-lipid pool interface. A thin flap of tissue (black arrowhead) can be seen over the cap. **(C)** Fly-through view (proximal to distal) shows a calcified lesion (black arrow) beneath a newly deployed stent. **(D)** OFDI cross-sectional image obtained at the location of the black arrow in (C) demonstrates a large calcific nodule (Ca) from 11–5 o'clock causing significant stent distortion, highlighted by the shorter inter-strut distances of the overlying stent compared to the opposing vessel wall. Color scale for (A) and (C): red—artery wall; green—

macrophages; yellow—lipid pool; blue—stent. Tick marks, 1 mm. (*) Denotes guide wire artifact.

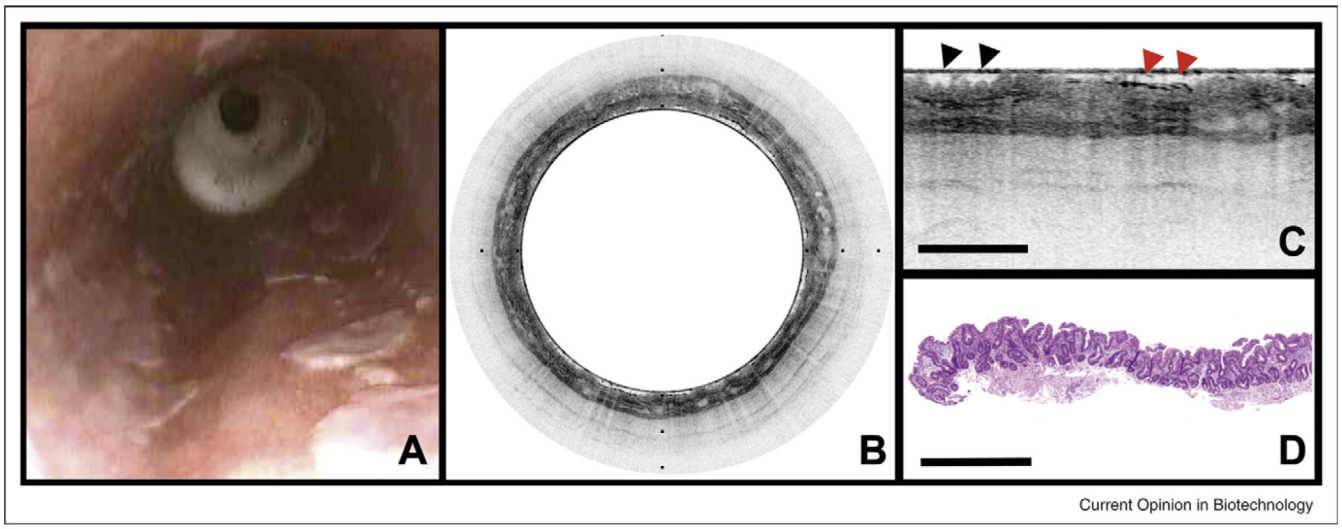

Figure 3.

OFDI images of human Barrett's esophagus, obtained *in vivo*. **(A)** Videoendoscope image shows islands of healthy squamous mucosa intermixed within regions of specialized intestinal metaplasia (SIM). **(B)** Circular transverse cross-sectional OFDI image with a layered appearance, and in some regions, an irregular surface and intraepithelial glands satisfying the OFDI diagnostic criterion of SIM. The 6 cm longitudinal segment was obtained in approximately 2 min at an acquisition rate of 9.8 frames per second (frame size: 2048 × 4096) and a pullback speed of 0.5 mm/s. **(C)** Expanded portion of (B) demonstrates surface irregularities (black arrowheads) and glands within the epithelium (red arrowheads). **(D)** Histopathologic image of the biopsy taken from the involved mucosa shows specialized and non-specialized columnar epithelium, consistent with the OFDI diagnosis of SIM. Scale bars and tick marks represent 1 mm.